

Detailed investigations on the effect of temperature and RF power on the optoelectronic properties of gallium doped zinc oxide thin films suitable for transparent conducting electrode applications

AROKIYADOSS RAYERFRANCIS, P. BALAJI BHARGAV*, K. GANESH KUMAR, NAFIS AHMED, C. BALAJI
SSN Research Centre, Sri Sivasubramaniya Nadar College of Engineering, Kalavakkam – 603110, India

Effect of substrate temperature and RF plasma power on the physical and optoelectronic properties of the RF magnetron sputtered GZO thin films is studied using suitable characterization techniques. 80% transmission is observed in the visible region and sheet resistance of the film observed to decrease from 2333.0 ohm/γ to 17.4 ohm/γ with increase in substrate temperature from room temperature to 250°C at 100 W power. Increasing power to 140 W resulted in the film with lowest sheet resistance of 6.2 ohm/sheet and conductivity of 1.23×10^{03} S/cm at 250°C substrate temperature. The potential of GZO as TCE is evaluated using FOM calculations.

(Received August 9, 2020; accepted June 11, 2021)

Keywords: GZO, XRD, FESEM, XPS, Optoelectronic properties, FOM

1. Introduction

High bandgap transition metal oxide materials with suitable doping are extensively used in various optoelectronic devices as Transparent Conducting Electrodes (TCEs) due to their moderately high electrical conductivity and high optical transmission in the visible region of the electromagnetic spectrum [1,2]. Furthermore, the transmission and conducting properties of these materials can be tuned by varying the dopant concentration [3]. Among various TCE materials, Indium Tin Oxide (ITO) is the most widely used material in various optoelectronic devices due to its superior electrical conductivity and optical transparency. But due to the scarcity of Indium and its instability in Silane plasma, especially in the case of thin film silicon solar cell fabrication by Plasma Enhanced Chemical Vapour Deposition (PECVD), there is a need to develop alternative TCE materials [4-8]. Among various alternatives, ZnO belonging to II-IV group, with a bandgap of ~3.37 eV and 60 meV of large exciton binding energy at room temperature [9-11], attracted the attention by various research groups due to its advantages such as stability in hydrogen and silane plasma, copiousness and non-toxic nature made it a viable alternative to ITO. We have already explored the transparent conducting properties of ZnO doped with Al (AZO) thin films and their applications in thin film silicon solar cells as TCE as well as back reflector [12-14]. Although Aluminium is extensively used in most of the research works as a dopant in ZnO, it is more reactive to Oxygen, which may lead to surface oxidation [15,16], thereby increasing the sheet resistance and resistivity. As Gallium is very less reactive to Oxygen, attention is being drawn by researchers to

optimize process parameters for the deposition of Ga doped ZnO to obtain suitable optoelectronic properties for various device applications [17,18]. Several techniques such as Metal-Organic Chemical Vapour Deposition (MOCVD), sputtering, spray pyrolysis and sol-gel are suitable for the deposition of Gallium doped ZnO (GZO) thin films [19-21]. Among all other available techniques, the films deposited using RF magnetron sputtering exhibit highly transparent and electrically conducting GZO thin films. Deposition of large area films at relatively low substrate temperature and good adhesion to the substrate are the added advantages of the sputtering technique.

In this particular work, highly conductive and transparent GZO films are grown by RF magnetron sputtering technique. The effect of substrate temperature and RF power on the structural, morphological, optical and electrical properties is investigated.

2. Experimental details

Transparent and conducting GZO films are deposited in an Ar atmosphere on Corning (Eagle Xg) glass substrates using RF magnetron sputtering system. Substrates are cleaned subsequently in acetone, isopropyl alcohol and finally in DI water by sonicating in an ultrasonic bath for 10 minutes each and dried with Nitrogen blow. A two-inch diameter GZO ceramic target ZnO (95 wt%): Ga₂O₃ (5 wt%) purchased from ITASCO, Korea is used for sputtering. Prior to deposition, the sputtering chamber is evacuated to 4×10^{-6} mbar using a rotary and diffusion pump combination to avoid oxygen and other contaminations if any during deposition. The working pressure is maintained at 0.01 mbar with a

constant Ar flow of 30 sccm. The substrate temperature is varied from R.T to 250°C and the RF power is maintained at 100 W (4.94 W/cm²). Effect of RF power on the film properties is also discussed. Substrate temperature (250°C), Argon flow rate (30 sccm), process pressure (0.01mbar) are kept constant. Various powers (power density) used for the GZO film deposition are 80 W (3.95 W/cm²), 100 W (4.94 W/cm²), 120 W (5.92 W/cm²) and 140 W (6.92 W/cm²).

The structure and crystalline nature of these films are explored by Seifert Analytical X-Ray diffractometer (XRD) using Cu-K α radiation with a wavelength of 0.15418 nm. The XPS spectra of the thin films are recorded using a PHI Model 5700 Multi-Technique system (monochromatized Al K α at $\nu = 1486.7$ eV). The thickness of the thin films is measured using a stylus profilometer (Dektak XT, Bruker). Electrical properties are evaluated using the Hall measurement system (HMS 5000, Ecopia). Optical transmission spectra are recorded using a UV-Visible spectrophotometer (Lambda 35, Perkin Elmer). The surface morphology and roughness of the thin films is analysed by field emission scanning electron microscope (FESEM) (Gemini, Zeis) and atomic force microscope (AFM) (Dimension V SPM, Veeco) respectively.

3. Results and discussion

The XRD pattern of GZO thin films deposited at various substrate temperatures is shown in Fig. 1. It is clearly shown that all the samples deposited at different temperatures exhibit a strong peak corresponding to (002) at 2 θ ~34° except for the film deposited at room temperature. The films are polycrystalline in nature, revealing the hexagonal wurtzite structure oriented along

the c-axis [22] whereas the film deposited at RT is amorphous in nature.

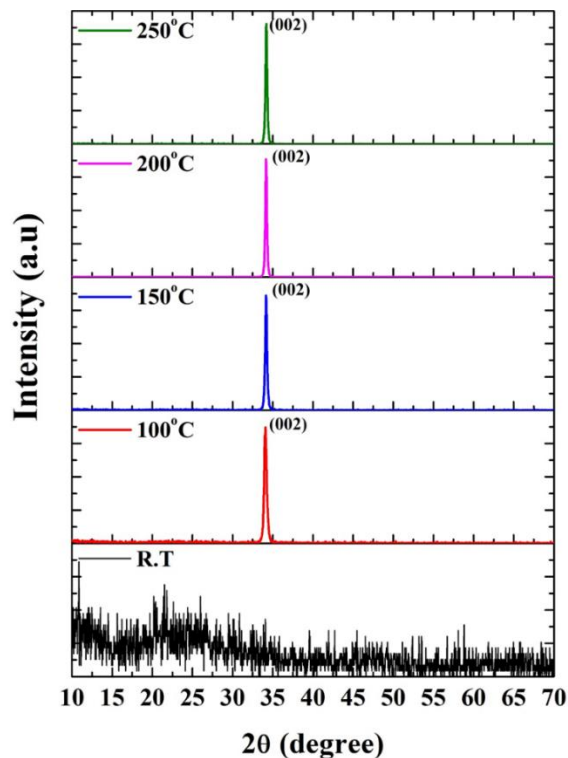


Fig. 1. XRD Pattern of GZO Thin Films Deposited at Various Substrate Temperatures with 100W RF power (color online)

Table 1. Structural Properties of GZO Thin Films Deposited at Different Substrate Temperatures with 100W RF Power

Substrate Temperature (°C)	FWHM (°)	Crystallite Size (nm)	“d” (Å)	“c” (Å)	“a” (Å)	V (Å) ³
R.T	--	--	--	--	--	--
100	0.397	21.88	2.63	5.26	3.22	47.13
150	0.299	28.99	2.62	5.24	3.21	46.82
200	0.275	31.60	2.62	5.24	3.21	46.82
250	0.258	33.65	2.62	5.24	3.21	46.70

We observe that the Bragg angle shift towards higher angles is observed with the increase of substrate temperature. As the substrate temperature increased, the peak intensity corresponding to the (002) plane increased considerably, due to the improvement in the crystallinity of the deposited films. The crystallite size calculated using the Sherrer formula,

$$D = \frac{0.9\lambda}{\beta \cos \theta}$$

The crystallite sizes of the films deposited at 100°C, 150°C, 200°C and 250°C are 21.88 nm, 28.99 nm, 31.6 nm and 33.65 nm, respectively. Along with the crystallite sizes, the value of ‘c’ in hexagonal wurtzite structure is

calculated using the formula from the XRD data of (002) plane,

$$\frac{1}{d^2} = \frac{4}{3} \left[\frac{h^2 + hk + k^2}{a^2} \right] + \frac{l^2}{c^2}$$

and the value of ‘a’ calculated from the c/a ratio (1.633). From these values, the volume of the cell was calculated using the formula,

$$V = 0.866 a^2 c$$

All these observed and calculated values of the GZO film deposited at different temperatures are given in table 1. In addition to the improvement in crystallite size, the cell volume of the ZnO hexagonal wurtzite structure

decreases with an increase in the substrate temperature. Hence it is proved that the substrate temperature plays an important role in the development of polycrystalline thin films using the sputtering technique. XRD patterns of the deposited films at different RF powers are shown in Fig. 2 and the FWHM and crystallite size calculated from the Scherrer formula and the other cell parameters such as 'a', 'c' and 'V' are given in Table 2.

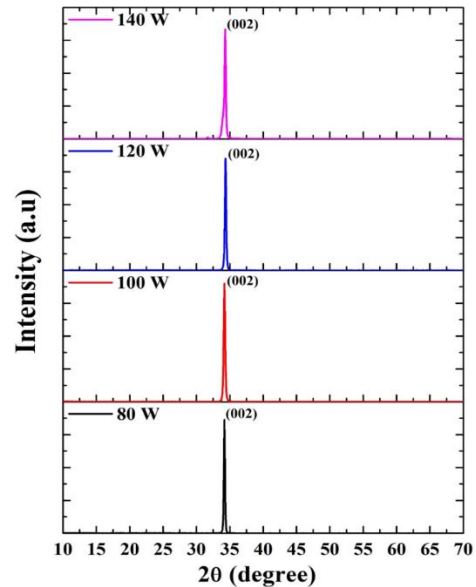


Fig. 2. XRD Pattern of GZO Thin Films Deposited at Various RF Powers at 250°C (color online)

Table 2. Structural Properties of GZO Thin Films Deposited at Different RF Power with 250°C Substrate Temperature

RF Power (W)	FWHM (°)	Crystallite Size (nm)	"d" (Å)	"c" (Å)	"a" (Å)	V (Å) ³
80	0.208	41.78	2.62	5.24	3.20	46.70
100	0.275	31.60	2.62	5.24	3.20	46.70
120	0.241	34.35	2.60	5.21	3.19	46.08
140	0.297	29.21	2.61	5.22	3.19	46.22

The deposited films are polycrystalline with hexagonal wurtzite structure and oriented along c-axis perpendicular to the substrate, exhibiting a single peak at $2\theta \sim 34^\circ$ corresponding (002) plane. The crystallinity of the GZO film does not show any consistent result with the RF power. Initially, the increase in the RF power favours the reduction in cell volume up to 120 W finally it slightly increased to 46.22 (Å)³ at 140W with increasing the RF power. This may be due to the rapid nucleation at the surface due to higher RF power.

XPS spectra of GZO thin films deposited using the RF magnetron sputtering technique are shown in Fig. 3. The peaks related to Zn2p_{3/2}, Zn2p_{1/2}, oxygen O1s, Ga2p are observed. The peaks at binding energies of 1021.4 eV and 1044.5 eV correspond to Zn 2p_{3/2} and Zn2p_{1/2}, respectively. The existence of a peak at a binding energy of 530.4 eV represents Oxygen O1s whereas the peaks at a binding energy of 1144.6 eV and 1117.8 eV confirm the presence of Ga2p_{1/2} and Ga2p_{3/2} [23]. This figure is representative of all the samples and is only used to confirm the existence of the constituent elements.

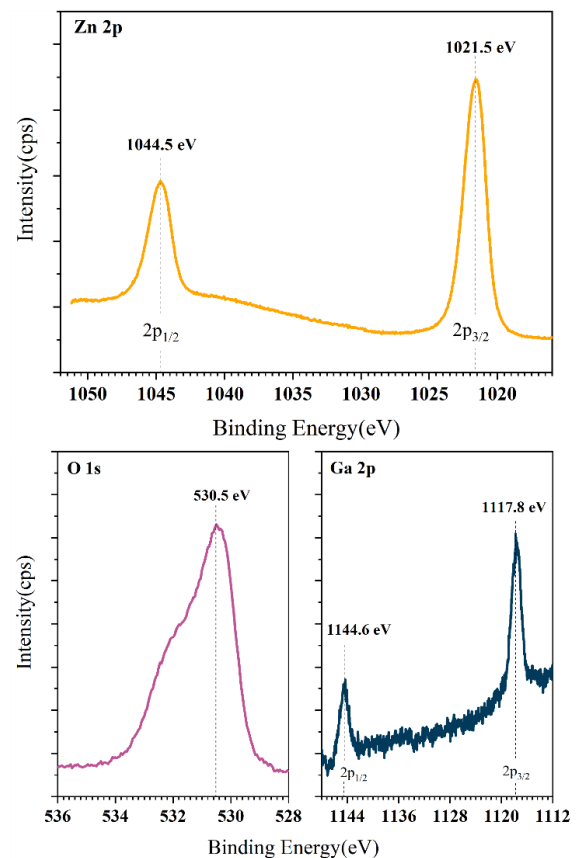


Fig. 3. XPS Spectra of GZO Thin Film deposited at 250°C and 100W power (color online)

2D and 3D AFM images of the GZO films deposited at R.T, 100°C, 150°C, 200°C and 250°C are shown in Figure 4. The Root Mean Square (RMS) roughness of the GZO films at room temperature is 4.83 nm and films deposited at higher temperatures is in the range of 13 nm to 20nm.

At 150°C, the RMS roughness increased to a maximum value of 20.1 nm which may be due to the abrupt clustering of grains leaving behind a relatively rough surface. Beyond this temperature, due to grain coalescence, the surface roughness decreased to 17 nm leaving relatively smoother surfaces. From the results, it is evident that roughness is sensitive to the substrate temperature.

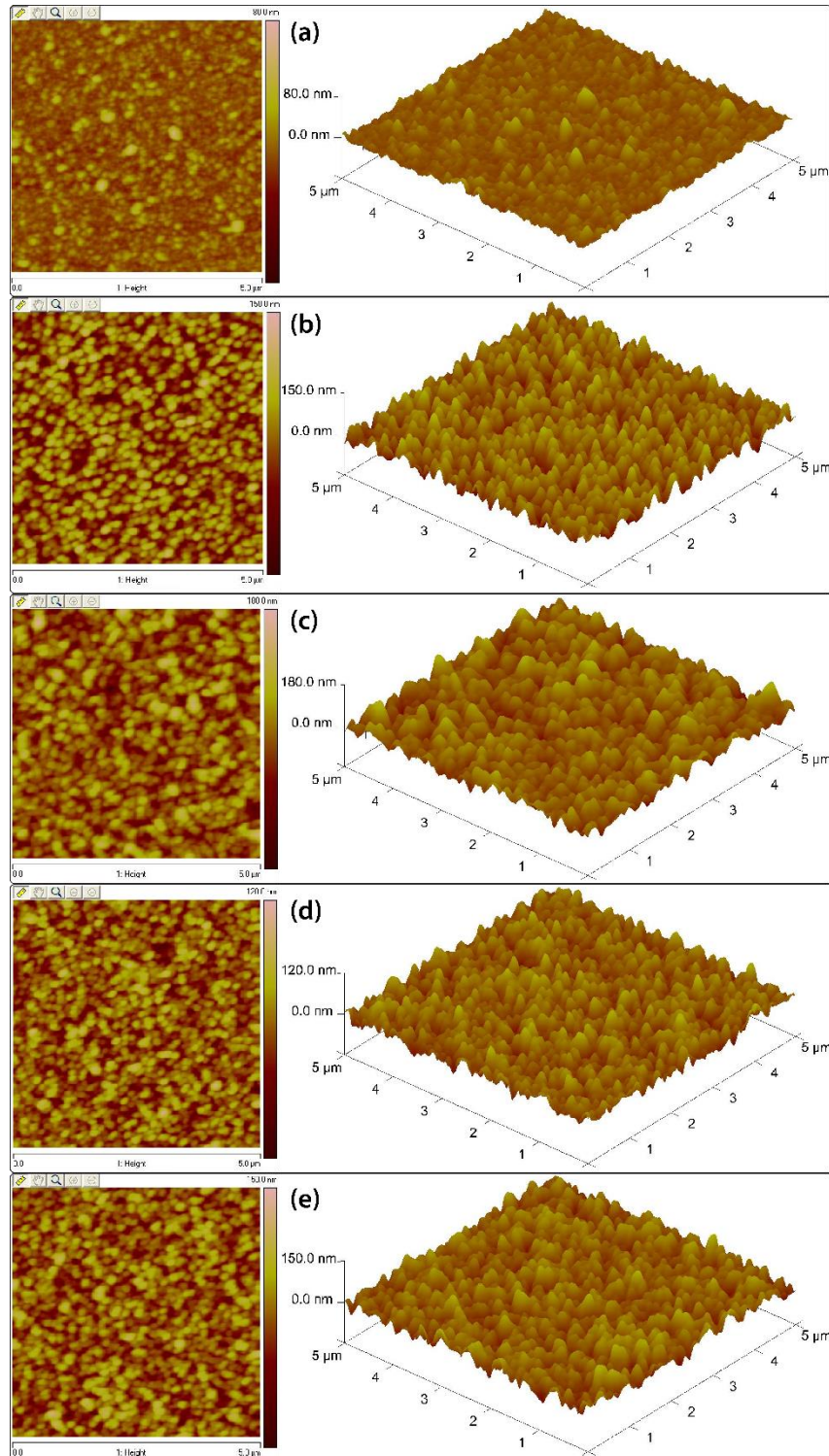


Fig. 4. AFM Image of GZO Thin Films Deposited at (a) R.T, (b) 100°C, (c) 150°C (d) 200°C and (e) 250°C with 100W RF Power (color online)

The AFM images of the GZO films deposited at different RF powers are shown in Fig. 5. The 2D and 3D image of each sample obtained from the AFM are given for better understanding. The RMS roughness of the film deposited at 80, 100, 120 and 140 Watts are 7.7, 17.0, 24.0 and 33.2 nm respectively. It can be seen from the figure, the surface roughness increases with an increase in the RF power. An increase in RF power yields columnar growth leading to the formation of larger grains, thereby increasing the surface roughness by a small fraction. This can be explained based on the trade-off between the rate of

film deposition and simultaneous damage of film surface by sputtered ions.

At lower RF power, the rate of film deposition prevails the incident sputtered ions bombardment of the film surface. Hence, we obtain a relatively smoother surface. When the RF power is increased, high energy incident ions outruns the rate of film deposition. This causes an increase in surface damage, thereby forming a slightly rough surface [24].

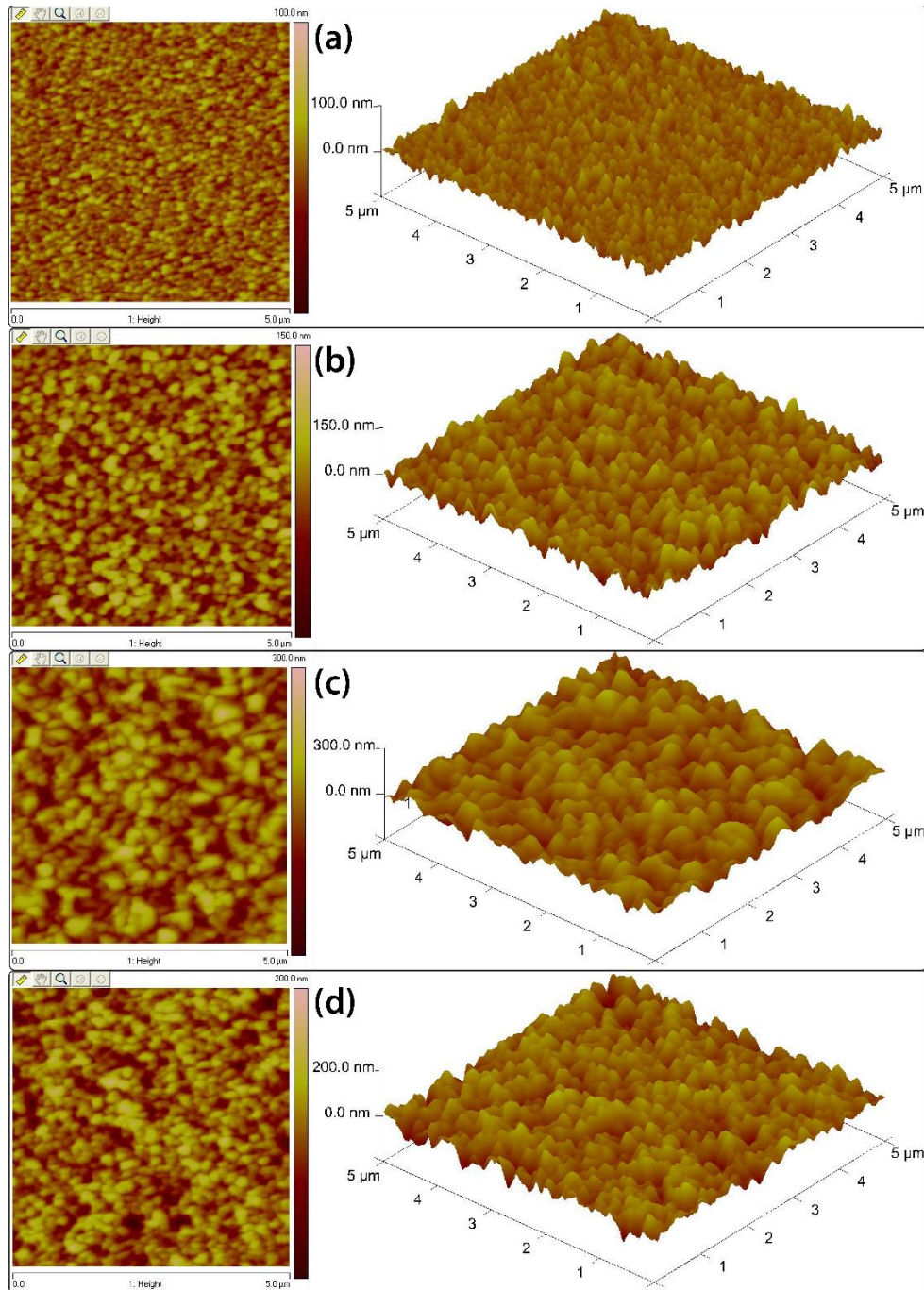


Fig. 5. AFM Image of GZO Thin Films Deposited at Different RF Powers: (a) 80 W, (b) 100 W, (c) 120 W and (d) 140 W with 250°C Substrate Temperature (color online)

The FESEM image of the GZO film deposited at various temperatures is given in Fig. 6. The surface morphology of the films deposited at R.T having particle kind of feature grown over the surface of the substrate. During sputter deposition, the film deposited at room temperature, the atoms and molecules are directly nucleated on the substrate and then grow into islands so that the ZnO molecules are more strongly bound to each other than to the substrate. This is because the energy of the sputtered species in the plasma is higher than the surface energy of the substrate. Volmer–Weber kind of growth takes place during this low temperature deposition and this results in an individual cluster kind of thin film [25]. As the substrate temperature increases, the

coalescence improves and the more continuous film is observed. The surface morphology of all GZO films except for GZO deposited at RT shows dense and compact surface features. The dense surface morphology of the films deposited at an elevated substrate temperature is due to the better surface interaction between the surface and the sputtered species.

FESEM images of the GZO thin films deposited at different RF power are given in Fig. 7. It is evident from the figure, the dimension of the hills and valleys become larger with increasing the RF power, which is in accordance with the RMS roughness obtained from the previous AFM study.

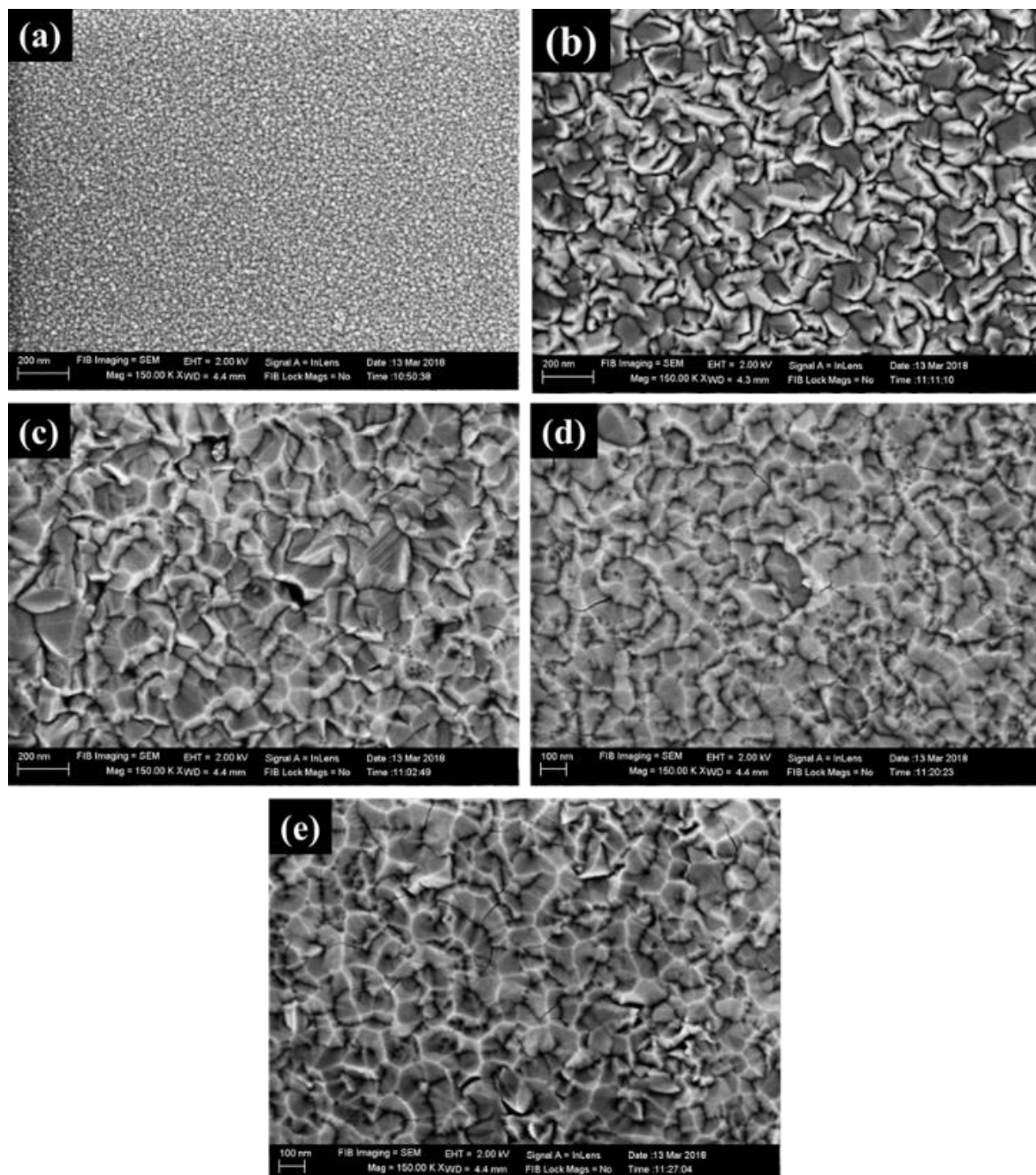


Fig. 6. FESEM Image of GZO Thin Films Deposited at (a)R.T, (b)100°C, (c)150°C, (d)200°C and (e)250°C with 100W RF Power

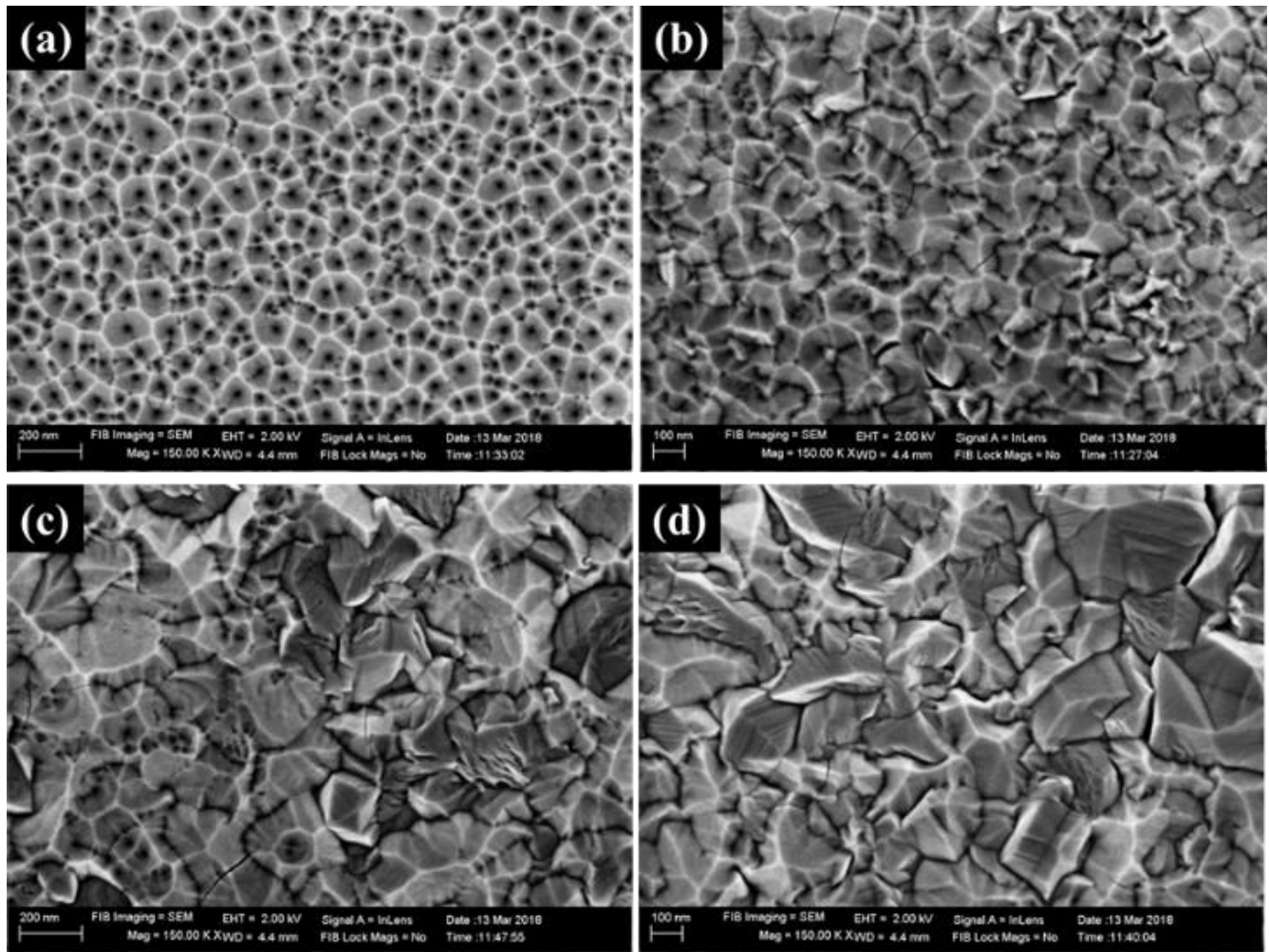


Fig. 7. FESEM Images of GZO Thin Films Deposited at Different RF Power: (a) 80 W, (b) 100 W, (c) 120 W and (d) 140 W with 250°C Substrate Temperature

The optical transmission spectra of the deposited GZO thin films are shown in Fig. 8. The overall transmission of the GZO films deposited at various substrate temperatures exhibits an average of 80% transmission in the visible region. At higher wavelengths, the transmission of the films deposited at a lower substrate temperature is more than the film deposited at higher substrate temperature. This is due to the increase of free electron concentration at high temperature deposited films and an increase in absorbance.

The bandgap (calculated from Tauc' plot) of the films deposited at R.T and 100°C are 3.24 eV and 3.25 eV, respectively and other films deposited at 150°C, 200°C and 250°C are ~3.39 eV. There is a slight variation in the transmission spectra of films deposited at 150°C, 200°C and 250°C temperatures but their band edge is similar in all cases. At higher deposition temperatures, larger amount of energy is delivered to the growing film resulting in reduction of structural light absorbing defects near the absorption edge, thereby increasing the optical bandgap of the film.

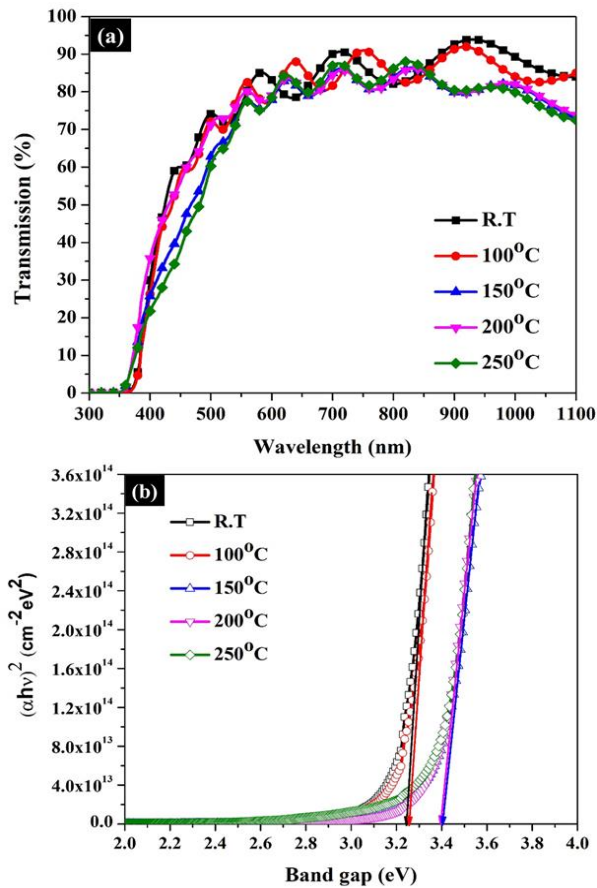


Fig. 8. (a) Transmission Spectra and (b) Bandgap Calculated from Tauc's Plot of GZO Thin Films Deposited at Different Substrate Temperatures with 100W RF Power (color online)

The transmission spectra of the GZO film deposited at different RF powers obtained from the UV-Vis spectrophotometer are presented in Fig. 9 (a). The average transmission of the films decreased with an increase in RF power. This is due to the increase in the thickness of the film. From Fig. 9 (b), the bandgap of the films calculated from the Tauc's plot are 3.33, 3.39, 3.30 and 3.42 eV for the RF power 80, 100, 120 and 140 Watt, respectively.

The thickness of the deposited GZO films is measured by a stylus profilometer. The film thickness is low at low substrate temperatures. With increasing the substrate temperature, the deposition rate increased to 6.84 nm/min at 150°C, with further increase in temperature the deposition rate is slightly reduced. The low thickness at lower substrate temperatures may be due to the poor surface adherence and re-sputtering from the substrate surface, the thickness increases with an increase in the temperature. Above 150°C the coalescence between the sputtered species at the substrate increases and packing of the film also increases as observed from the FESEM images.

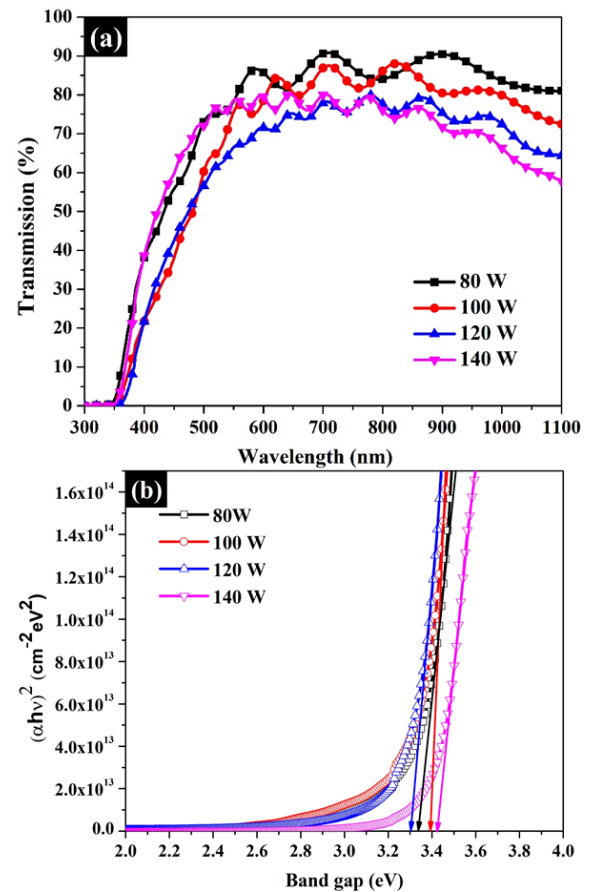


Fig. 9. (a) Transmission Spectra and (b) Bandgap Calculated from Tauc's Plot of GZO Thin Films Deposited at Different RF Power with 250°C Substrate Temperature (color online)

The electrical properties of the GZO films such as carrier concentration, sheet resistance, resistivity, conductivity are improved with an increase in the substrate temperature (Table 3). The pure ZnO film has very high sheet resistance and poor conductivity as reported earlier [26]. The carrier concentration of pure ZnO is in the order of 10^{17} cm^{-3} and by doping got increased to $\sim 10^{18} \text{ cm}^{-3}$ for the film deposited at the room temperature and to $\sim 10^{20} \text{ cm}^{-3}$ at 250°C. The sheet resistance reduced from 2.3 K Ω/\square to 17.4 Ω/\square , resistivity reduced from $1.15 \times 10^{-01} \Omega\text{-cm}$ to $1.49 \times 10^{-03} \Omega\text{-cm}$ and the conductivity increased from 8.65 to $6.67 \times 10^{02} \text{ S/cm}$. The increase in surface temperature causes the reduction in structural defects and grain boundaries which yields an increase in conductivity.

Increasing the RF power increases the sputtering yield, which causes an increase in the thickness of the GZO film. The electrical properties of GZO thin films analysed using the Hall measurement system and the results are given in Table 4.

The carrier concentration of the GZO thin film increased from $\sim 10^{19}$ to $\sim 10^{21} \text{ cm}^{-3}$ with the RF power increased from 80 W to 140 W. The carrier concentration of the film deposited at 80 W is $6.54 \times 10^{19} / \text{cm}^3$ with a mobility value of 75.7 $\text{cm}^2/\text{V.s}$ and the carrier concentration is increased to a maximum value of $1.05 \times 10^{21} / \text{cm}^3$ for 140 W with the minimum mobility of 7.3. The decrease in mobility may be due to the increase in carrier concentration.

Table 3. Electrical properties and FOM of GZO thin films deposited at different substrate temperatures with 100W RF power

Substrate Temperature (°C)	Carrier Concentration (cm ⁻³)	Sheet Resistance (Ω/□)	Conductivity (S/cm)	Mobility (cm ² /V.s)	Dep. Rate (nm/min)	FOM (Ω ⁻¹)
RT	2.21×10 ¹⁸	2333.0	8.65×10 ⁰⁰	24.4	4.34	3.25×10 ⁻⁴
100	3.33×10 ¹⁹	231.9	1.56×10 ⁰²	29.3	5.17	3.49×10 ⁻³
150	4.98×10 ¹⁹	143.6	1.39×10 ⁰²	17.4	6.84	5.22×10 ⁻³
200	3.36×10 ¹⁹	62.6	3.21×10 ⁰²	59.4	6.69	1.24×10 ⁻²
250	1.33×10 ²⁰	17.4	6.67×10 ⁰²	31.3	6.43	4.31×10 ⁻²

Table 4. Electrical properties and FOM of GZO thin films deposited at different RF power with 250oC substrate temperature

Power (W)	Carrier Concentration (cm ⁻³)	Sheet Resistance (Ω/□)	Conductivity (S/cm)	Mobility (cm ² /V.s)	Dep. Rate (nm/min)	FOM (Ω ⁻¹)
80	6.54×10 ¹⁹	25.0	7.94×10 ⁰²	75.7	4.75	3.12×10 ⁻²
100	1.33×10 ²⁰	17.4	6.67×10 ⁰²	31.3	6.43	4.31×10 ⁻²
120	2.55×10 ²⁰	15.8	6.01×10 ⁰²	14.6	7.91	4.17×10 ⁻²
140	1.05×10 ²¹	6.2	1.23×10 ⁰³	7.3	10.07	1.25×10 ⁻²

The lowest sheet resistance of 6.2 Ω/γ is obtained at 140 W with high carrier concentration which is suitable for TCE applications in various optoelectronic devices [27].

The figure of merit (FOM) value of transparent electrode, as suggested by Haccke [26, 28], provides useful information for comparing the performance of transparent conducting electrodes when their optical transmission and electrical sheet resistance are known. It is calculated using the equation, $\phi_{TC} = T^{10}/R_s$. FOM of GZO thin films deposited at different substrate temperatures and RF power is given in Table 3 and Table 4, respectively. The lowest value (0.3×10⁻³ Ω⁻¹) of FOM was observed in the GZO film deposited at room temperature and increased with an increase in the substrate temperature. This increment in FOM is due to the decrease in sheet resistance of the GZO film with increasing the substrate temperature. A maximum of 43×10⁻³ Ω⁻¹ is obtained with the substrate temperature of 250°C. The FOM of GZO film deposited at 80 W is 31×10⁻³ Ω⁻¹, increased to 125×10⁻³ Ω⁻¹ for the film deposited at 140 W. This is again due to the decrease in sheet resistance of the GZO thin film with the increase in RF power.

4. Conclusion

Gallium doped Zinc oxide (GZO) thin films are deposited using the RF magnetron sputtering technique. Effect of substrate temperature and the RF power on the structural, morphological, optical and electrical properties is investigated. Structural properties of the deposited thin films are analysed using the XRD pattern. The thin film deposited at room temperature does not have any crystalline property. With an increase in substrate temperature, the crystallinity of the thin films improved. The crystallite size increased from 21.88 nm for the film deposited at 100°C to 33.65 nm for the film deposited at 250°C. The surface morphology of the deposited films is

analysed using AFM and FESEM. The RMS roughness varied between 4.83 nm and 20.1 nm with the increase of substrate temperature and increased from 7.7 nm to 33.2 nm by increasing the RF power from 80W to 140 W. Transmission property of the films studied using UV-Visible spectrophotometer and the observed transmission is more than 80% in the visible region which increases with an increase in the substrate temperature and decreases with an increase in the RF power. The deposited GZO thin films have a wide bandgap of more than 3.3 eV, calculated using Tauc's plot. The most important electrical parameters such as carrier concentration, sheet resistance, resistivity, conductivity and mobility are obtained from the Hall measurement system. GZO thin films with more than 85% transmission, 6.2 Ω/□ sheet resistance and 8.13×10⁻⁰⁴ Ω cm resistivity is achieved. The optimised GZO thin films deposited by RF magnetron are suitable for TCE and back reflector applications in thin films solar cells.

Acknowledgements

The author Arokiyadoss Rayerfrancis would like to thank the financial support from SSN Trust.

References

- [1] D. Levy, E. Castellon, Transparent Conductive Materials, Wiley-VCH, 2008.
- [2] T. Koida, Y. Ueno, J. Nishinaga, Y. Kamikawa, H. Higuchi, M. Iioka, Thin Solid Films **673**, 26 (2019).
- [3] A. Klein, C. Körber, A. Wachau, F. Säuberlich, Y. Gassenbauer, S. Harvey, Materials **3**, 4892 (2010).
- [4] K. Ellmer, A. Klein, B. Rech, Transparent conductive zinc oxide, Springer, Berlin, 2008.
- [5] S. Lee, H. Cho, G. Panin, T. Won Kang, Applied Physics Letters **98**, 093110 (2011).

- [6] G. Li, J. Song, J. Zhang, X. Hou, *Solid-State Electronics* **92**, 47 (2014).
- [7] S. Okuda, T. Matsuo, H. Chiba, T. Mori, K. Washio, *Thin Solid Films* **557**, 197 (2014).
- [8] R. Khokhra, B. Bharti, H. Lee, R. Kumar, *Scientific Reports* **7**, 15032 (2017).
- [9] B. Choi, H. Im, J. Song, K. Yoon, *Thin Solid Films*, **193-194**, 712-720, (1990).
- [10] T. Andrearczyk, J. Jaroszyński, G. Grabecki, T. Dietl, T. Fukumura, M. Kawasaki, *Physical Review B* **72**(12), 121309 (2005).
- [11] X. Li, H. Li, Z. Wang, H. Xia, Z. Xiong, J. Wang, *Optics Communications* **282**, 247 (2009).
- [12] A. Rayerfrancis, P.B. Bhargav, N. Ahmed, S. Bhattacharya, B. Chandra, S. Dhara, *Silicon* **9**, 31 (2017).
- [13] S. Bose, A. Rayerfrancis, P. Balaji Bhargav, G. Ahmad, S. Mukhopadhyay, S. Mandal, *Journal of Materials Science: Materials In Electronics* **29**, 3210 (2017).
- [14] A. Rayerfrancis, P. Balaji Bhargav, N. Ahmed, C. Balaji, G. Kumar, *Materials Letters* **221**, 305 (2018).
- [15] K. Manjunatha, S. Paul, *Applied Surface Science* **424**, 316 (2017).
- [16] T. Prasada Rao, C. Santhosh Kumar, *Journal of Crystallization Process and Technology* **02**, 72 (2012).
- [17] H. Park, J. Kang, S. Na, D. Kim, H. Kim, *Solar Energy Materials and Solar Cells* **93**(11), 1994 (2009).
- [18] E. Ratcliff, A. Sigdel, M. Macech, K. Nebesny, P. Lee, D. Ginley, N. Armstrong, J. Berry, *Thin Solid Films* **520**(17), 5652 (2012).
- [19] H. An, H. Ahn, J. Park, *Ceramics International* **41**(2), 2253 (2015).
- [20] S. Appani, S. Rayapati, D. Sutar, S. Major, *AIP Conference Proceedings* **1942**, 120009 (2018).
- [21] J. Yang, Y. Jiang, L. Li, M. Gao, *Applied Surface Science* **421**, 446 (2017).
- [22] F. Wang, C. Huang, C. Yang, H. Tzeng, *International Journal of Photoenergy* **2013**, 270389.1-7 (2013).
- [23] F. Wang, K. Chen, C. Hsu, M. Liu, C. Yang, *Nanomaterials* **6**(5), 88 (2016).
- [24] Chuen-Lin Tien, Kuo-Chang Yu, Tsung-Yo Tsai, Ming-Chung Liu, *Applied Surface Science* **354**, 79 (2015).
- [25] J. A. Venables, G. D. T. Spiller, *NATO Advanced Science Institutes Series (Series B: Physics)*, **86**, Springer, Boston, MA, 1983.
- [26] A. Rayerfrancis, P.B. Bhargav, N. Ahmed, C. Balaji, G. Kumar, *The European Physical Journal Applied Physics* **82**(2), 20301 (2018).
- [27] S. Bikash, Dipak Barman, Bimal K. Sarma, *Applied Surface Science* **479**(15), 786 (2019).
- [28] G. Haacke, *Journal of Applied Physics*, **47**(9), 4086 (1976).

*Corresponding author: balajibhargavp@ssn.edu.in